

# Resolved $\gamma_L^*$ in hard collisions of virtual photons: QCD effects

Jiří Chýla and Marek Taševský<sup>a</sup>

Institute of Physics of the Academy of Sciences of the Czech Republic  
Na Slovance 2, Prague 8, Czech Republic

Received: date / Revised version: date

**Abstract.** The manifestations of QCD effects on quark and gluon distribution functions of longitudinally polarized virtual photons involved in hard collisions are investigated. It is shown that for moderate photon virtualities and in the kinematical region accessible at HERA and LEP these effects are sizable and significantly enhance theoretical predictions based on contributions of transversally polarized virtual photon only.

## 1 Introduction

In QED quantized in covariant gauge, longitudinally polarized on-shell photons are present, but due to gauge invariance decouple, order by order in perturbation theory, in expressions for physical quantities. For the virtual photon with virtuality  $^1 P^2$  its longitudinal polarization, denoted  $\gamma_L^*$ , does contribute to physical quantities and gauge invariance merely requires that these contributions vanish as  $P^2 \rightarrow 0$ . In a previous publication [1] we have discussed the contributions of  $\gamma_L^*$  to two physical quantities using purely QED formula for quark distribution functions of  $\gamma_L^*$ . In this paper we continue our investigation of the relevance of  $\gamma_L^*$  in hard collisions by incorporating the effects of QCD radiation on parton distribution functions (PDF) of  $\gamma_L^*$  recently derived in [2]. In the next Section the rationale for introducing the concept of the structure of virtual photon is recalled, followed in Sections 3 and 4 by a short review of the QED and QCD formulae for corresponding PDF. The numerical relevance of the contributions of resolved  $\gamma_L^*$  with QCD improved PDF are discussed in Sections 5 for the LO and in Section 6 for the NLO QCD calculations.

## 2 Virtual photon and its “structure”

Let us briefly recall the virtue of extending the concept of partonic “structure” to virtual photons [3,5]:

- In principle, the concept of partonic structure of virtual photons can be dispensed with as higher order

<sup>a</sup> Work done within the *Center for Particle Physics* under the project LN00A006 of the Ministry of Education of the Czech Republic.

<sup>1</sup> In this paper the virtuality of a particle with four-momentum  $k$  and mass  $m$  is defined as  $|k^2 - m^2|$ .

QCD corrections to cross sections of processes involving virtual photons in the initial state are well-defined and finite even for massless partons.

- In practice, however, the concept of *resolved virtual photon* is extraordinarily useful as it allows us to include the resummation of higher order QCD effects that come from physically well-understood region of (almost) parallel emission of partons off the quark or antiquark coming from the primary  $\gamma^* \rightarrow q\bar{q}$  splitting.

For the virtual photon, as opposed to the real one, its PDF <sup>2</sup> can therefore be regarded as “merely” describing higher order perturbative effects and not its “genuine” structure. Although this distinction between the content of PDF of real and virtual photons exists, it does not affect the extraordinary *phenomenological* usefulness of PDF of the virtual photon. As shown in [3] the nontrivial part of the contributions of resolved transverse virtual photon ( $\gamma_T^*$ ) to NLO calculations of dijet production at HERA is large and affects significantly the conclusions of phenomenological analyses of existing experimental data.

## 3 PDF of $\gamma_L^*$ in QED

Most of the present knowledge of the structure of the photon comes from experiments at ep and  $e^+e^-$  colliders, where the incoming leptons act as sources of transverse and longitudinal virtual photons of virtuality  $P^2$  and momentum fraction  $y$ . To order  $\alpha$  their respective unintegrated fluxes are given as

$$f^{\gamma_T^*}(y, P^2) = \frac{\alpha}{2\pi} \left( \frac{1 + (1-y)^2}{y} \frac{1}{P^2} - \frac{2m_e^2 y}{P^4} \right), \quad (1)$$

$$f^{\gamma_L^*}(y, P^2) = \frac{\alpha}{2\pi} \frac{2(1-y)}{y} \frac{1}{P^2}. \quad (2)$$

<sup>2</sup> More precisely their pointlike parts.

Phenomenological analyses of interactions of virtual photons and their PDF have so far concentrated on its transverse polarization. Neglecting longitudinal photons is a good approximation for  $y \rightarrow 1$ , where  $f^{\gamma_L^*}(y, P^2) \rightarrow 0$ , as well as for small virtualities  $P^2$ , where PDF of  $\gamma_L^*$  vanish by gauge invariance. But how small is “small” in fact? For instance, should we take into account the contribution of  $\gamma_L^*$  to jet cross-section in the region  $E_T \gtrsim 5$  GeV,  $P^2 \gtrsim 1$  GeV<sup>2</sup>, where most of the data on virtual photons obtained in ep collisions at HERA come from? The present paper is devoted to addressing this and related questions.

In pure QED and to order  $\alpha$  the probability of finding inside  $\gamma_L^*$  of virtuality  $P^2$  a quark with mass  $m_q$ , charge  $e_q$ , momentum fraction  $x$  and virtuality  $\tau \leq M^2$ , is given, in units of  $3e_q^2\alpha/2\pi$ , as [3]

$$q_L^{\text{QED}}(x, m_q^2, P^2, M^2) = \frac{4x^2(1-x)P^2}{\tau^{\min}} \left(1 - \frac{\tau^{\min}}{M^2}\right), \quad (3)$$

where  $\tau^{\min} = xP^2 + m_q^2/(1-x)$ . The quantity defined in (3) has a clear physical interpretation: it describes the flux of quarks that are almost collinear with the incoming photon and “live” longer than  $1/M$ . For  $\tau^{\min} \ll M^2$  the expression (3) simplifies to

$$q_L^{\text{QED}}(x, m_q^2, P^2, M^2) = \frac{4x^2(1-x)P^2}{xP^2 + m_q^2/(1-x)},$$

which for  $x(1-x)P^2 \gg m_q^2$  further reduces to

$$q_L^{\text{QED}}(x, 0, P^2, M^2) = 4x(1-x). \quad (4)$$

whereas for  $x(1-x)P^2 \ll m_q^2$

$$q_L^{\text{QED}}(x, m_q^2, P^2, M^2) \rightarrow \frac{P^2}{m_q^2} 4x^2(1-x)^2$$

demonstrating the fact that in QED the onset of  $\gamma_L^*$  is governed by the ratio  $P^2/m_q^2$ .

## 4 QCD improved PDF of $\gamma_L^*$

QCD improved PDF of  $\gamma_L^*$  have been derived in the leading-logarithmic approximation and for  $1 \lesssim P^2 \ll M^2$  in [2]. By “leading-log” we mean resummation of the terms  $(\alpha_s \ln M^2)^k$  at each order  $k$  of perturbative QCD. Note that for  $\gamma_T^*$  there is one power of  $\ln M^2$  more at each order of  $\alpha_s$ , the additional one coming from the primary QED  $\gamma^* \rightarrow q\bar{q}$  splitting. In the case of  $\gamma_L^*$  the analogous splitting gives rise to the term (4), which is constant in  $P^2$ . The resulting expressions<sup>3</sup> exhibit typical hadronic form of scale dependence and contain  $\Lambda_{\text{QCD}}$  as the only free parameter. The condition  $P^2 \ll M^2$  guarantees clear physical meaning of the resulting quark and gluon distribution functions. Moreover, by staying away from the

region  $P^2 \sim M^2$  we avoid the region where power corrections of the type  $P^2/M^2$  are essential and, in fact, more important than the effects described by PDF. The restriction from below  $1 \text{ GeV}^2 \lesssim P^2$  ensures that hadronic parts of PDF of  $\gamma_L^*$ , which have not been taken into account in the derivation in [2], can be safely neglected with respect to the pointlike ones<sup>4</sup>.

The relevance of resolved  $\gamma_L^*$  in hard collisions of virtual photons<sup>5</sup> depends on the theoretical framework one works in. In the next two Sections we shall discuss the effects of including resolved  $\gamma_L^*$  within the LO as well as NLO QCD calculations. The difference between the numerical relevance of resolved  $\gamma_L^*$  in these two cases arises from the fact that parton level calculations contain at the order  $\alpha^2\alpha_s^2$  some of the effects that go into the definitions of quark distribution function of  $\gamma_T^*$  and  $\gamma_L^*$ .

## 5 Resolved $\gamma_L^*$ in LO QCD calculations

### 5.1 DIS on $\gamma^*$

In LO QCD the structure function  $F_2^\gamma$  of the virtual photon is given in terms of quark distribution functions by the same expression as for hadrons<sup>6</sup>

$$F_2^\gamma(x, P^2, Q^2) = \sum_i 2xe_i^2 (q_i(x, P^2, Q^2) + \bar{q}_i(x, P^2, Q^2)).$$

<sup>4</sup> This claim is based on experience with SaS sets of parameterizations [4] and the assumption that hadronic parts of PDF of  $\gamma_L^*$  can be related to those of  $\gamma_T^*$  [2].

<sup>5</sup>  $\gamma_L^*$  contributes to soft collisions and related quantities, like  $\sigma_{\text{tot}}(\gamma^*p)$ , as well, but we restrict our discussion to hard collisions. For the former, the reader is referred to [6].

<sup>6</sup> We disregard the consequences of the reformulation of QCD analysis of  $F_2^\gamma$  proposed by one of us in [7] as they do not concern the main point of our discussion.

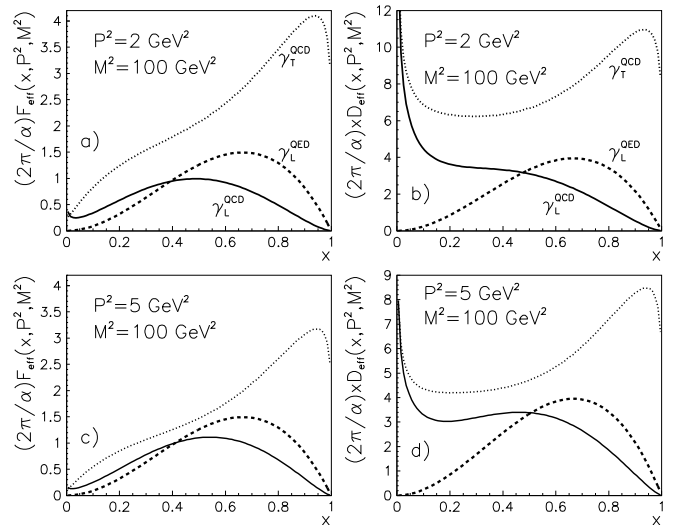


**Fig. 1.** Comparison of the contributions of  $\gamma_T^*$  and  $\gamma_L^*$  to  $F_{\text{eff}}^\gamma$  (left) and  $D_{\text{eff}}$  (right) for  $P^2 = 2, 5$  GeV<sup>2</sup> and  $M^2 = 100$  GeV<sup>2</sup>.

<sup>3</sup> The parameterization of PDF of  $\gamma_L^*$  can be obtained from chyla@fzu.cz.

In all existing phenomenological analyses only target  $\gamma_T^*$  has been taken into account, despite the fact that for  $P^2 \ll Q^2$  experiments at LEP [8,9] actually measure <sup>7</sup> the “effective” structure function

$$F_{\text{eff}}^\gamma(x, P^2, Q^2) \equiv F_{2,T}^\gamma(x, P^2, Q^2) + F_{2,L}^\gamma(x, P^2, Q^2)$$

given as the sum of contributions from target  $\gamma_L^*$  and  $\gamma_T^*$ . In Fig. 1a,c we compare, for two pairs of  $P^2$  and  $Q^2$  typical for current experiments at LEP,  $F_2^\gamma$  obtained with SaSID parameterization [4] of PDF of  $\gamma_T^*$  with the contributions from target  $\gamma_L^*$  evaluated using both the QED and QCD expressions for  $q_L(x, P^2, M^2)$  discussed in the preceding two Sections. The contributions from  $q_L^{\text{QED}}$  peak around  $x \simeq 0.7$ , with QCD effects suppressing them at large  $x$  and enhancing them on the other hand for  $x \lesssim 0.4$ . The presence of the term proportional to  $\ln M^2$  in the expression for  $q_T$  in both QED and QCD implies the dominance of  $\gamma_T^*$  at large  $M^2$ , but one would have to go to very large  $M^2$  for  $\gamma_L^*$  to become negligible with respect to  $\gamma_T^*$ . For fixed  $M^2$  the relative importance of  $\gamma_L^*$  with respect to  $\gamma_T^*$  grows with  $P^2$ , but to retain clear physical meaning of PDF we stay throughout this paper in the region  $P^2 \ll M^2$ .

## 5.2 Dijet production in ep collisions

The measurement of dijet production in ep collisions provides another way of investigating interactions of virtual photons [10,11]. In general the corresponding cross sections are given as sums of contributions of all possible parton level subprocess. The simplest way of demonstrating the importance of contributions of resolved  $\gamma_L^*$  employs the approximation [12] in which dijet cross sections are expressed in terms of a single *effective parton distribution function* of the photon (either  $\gamma_T^*$  or  $\gamma_L^*$ ) defined as

$$D_{\text{eff}}(x, P^2, M^2) \equiv \sum_{i=1}^{n_f} (q_i(x, P^2, M^2) + \bar{q}_i(x, P^2, M^2)) + \frac{9}{4}G(x, P^2, M^2),$$

where the factorization scale  $M$  is conventionally identified with (a multiple of) jet  $E_T$ :  $M = \kappa E_T$ . In Figs. 1b,d the contributions to  $D_{\text{eff}}$  from  $\gamma_T^*$  and  $\gamma_L^*$  are compared for two pairs of  $P^2$  and  $M^2$  typical for HERA experiments. In addition to effects at large  $x$ , which are similar to those for  $F_{\text{eff}}^\gamma$ ,  $D_{\text{eff}}$  gets a sizable contribution from  $\gamma_L^*$  at small  $x$ , coming from its gluon content. The rise of  $D_{\text{eff}}$  at small  $x$  is particularly clear effect of QCD improved PDF of  $\gamma_L^*$ . After this estimate, we now proceed to discuss the contributions of  $\gamma_L^*$  to dijet cross sections evaluated with HERWIG 5.9 event generator at the parton level. We could have used for this purpose also JETVIP [13], which we shall use later at the NLO, but using HERWIG at the LO allows us to

- estimate hadronization effects,

<sup>7</sup> Neglecting the difference of the fluxes (1-2), which is a good approximation at small  $y$ , typical for LEP experiments.

- cross-check the modifications implemented in JETVIP in order to include the effects of  $\gamma_L^*$ .

For the purpose of this study we have modified standard HERWIG 5.9 by adding the option of generating the flux of  $\gamma_L^*$  combined with the call to QED or QCD improved PDF of  $\gamma_L^*$ . For  $\gamma_T^*$  the SaSID PDF were used. All calculations were performed for  $0.05 \leq y \leq 0.95$ , three windows of  $P^2$ :  $1.4 \leq P^2 \leq 2.4 \text{ GeV}^2$ ,  $2.4 \leq P^2 \leq 4.4 \text{ GeV}^2$  and  $4.4 \leq P^2 \leq 10 \text{ GeV}^2$  and the following cuts on parton  $E_T$

$$E_T^{(1)}, E_T^{(2)} \geq E_T^c, \quad E_T^c = 5, 10 \text{ GeV}.$$

The effects of H1 and ZEUS detector acceptances have been approximately taken into account by performing all calculations without any restriction on parton pseudorapidity as well as for  $-3 \leq \eta \leq 0$ .

The results for the first window in  $P^2$  and without the cuts on  $\eta$  are presented as functions of  $\eta$ ,  $x_\gamma$  and  $E_T$  in Fig. 2. The characteristic dependence of the contributions of resolved  $\gamma_L^*$  on  $y$  is illustrated by plotting for each of the distributions in  $\eta$ ,  $E_T$  and  $x_\gamma$  also its ratio to that of  $\gamma_T^*$  for the whole interval  $0.05 \leq y \leq 0.95$ , as well as for three indicated subintervals. Except for  $x_\gamma$  close to 1, QCD improved PDF of  $\gamma_L^*$  enhance its contributions to dijet cross sections compared to those based on the purely QED. For  $y \lesssim 0.5$  and  $x_\gamma$  close to 0 or  $\eta \simeq 2.5$ , the contributions of resolved  $\gamma_L^*$  amount to about 80% of those of  $\gamma_T^*$ , whereas on average this number is around 50%. Reducing the range of  $\eta$  to  $-3 \leq \eta \leq 0$  affects (see Fig. 3) mainly the distribution  $d\sigma/dx_\gamma$  by suppressing it at both endpoints  $x_\gamma = 0$  and  $x_\gamma = 1$ . The ratios of the contributions of  $\gamma_L^*$  and  $\gamma_T^*$  are, however, affected only little by this cut. Increasing the photon virtuality enhances, as shown in Fig. 4, the relative importance of resolved  $\gamma_L^*$  with respect to  $\gamma_T^*$ . On the contrary, rising the threshold  $E_T^c$  from 5 GeV to 10 GeV reduces it, as illustrated in Fig. 5, by a factor of about 2, since large  $E_T$  require large  $x_\gamma$ , where quarks from  $\gamma_T^*$  dominate.

Summarizing the message of Figs. 2-4, we conclude that in the region  $\Lambda^2 \ll P^2 \ll M^2 \approx E_T^2$  the contributions of  $\gamma_L^*$  are substantial, particularly for

- small  $y$ ,
- low  $E_T$ ,
- $x_\gamma \lesssim 0.5$ , corresponding to  $\eta$  close to the upper edge.

The cuts enforced by H1 and ZEUS acceptances reduce the sensitivity to  $\gamma_L^*$ , but its contributions still make up typically 30 – 50% of those of  $\gamma_T^*$  and can be identified by their characteristic  $y$  and  $P^2$  dependencies.

## 6 Resolved $\gamma_L^*$ in NLO QCD calculations

The relevance of resolved  $\gamma_L^*$  within the framework of NLO parton level calculations of dijet cross sections in ep collisions has been investigated using JETVIP [13], the only NLO parton level MC program including both direct and resolved photon contributions. In specifying the powers of  $\alpha$  and  $\alpha_s$  corresponding to various Feynman diagrams

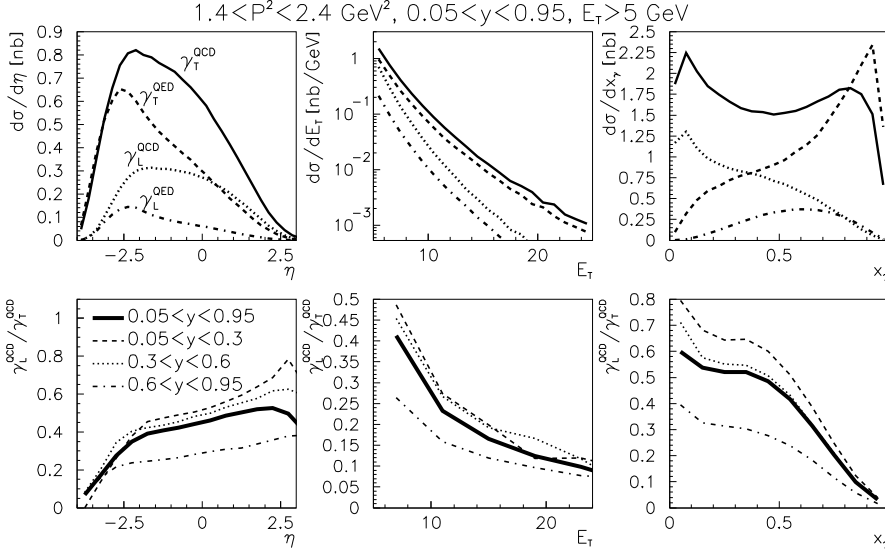


**Fig. 2.** Upper three plots: diparton cross sections, corresponding to target  $\gamma_T^*$  and  $\gamma_L^*$  and using QED as well as QCD improved PDF of the latter, plotted as functions of  $\eta$ ,  $E_T$  and  $x_\gamma$  for  $1.4 \leq P^2 \leq 2.4$  GeV<sup>2</sup>,  $0.05 \leq y \leq 0.95$ ,  $E_T \geq 5$  GeV, without any restriction on  $\eta$ . Lower three plots: ratio of the contributions of resolved  $\gamma_L^*$  (using PDF of [2]) to those of  $\gamma_T^*$  (evaluated with PDF of [4]), integrated over the whole region  $0.05 \leq y \leq 0.95$ , as well as in three indicated subintervals.

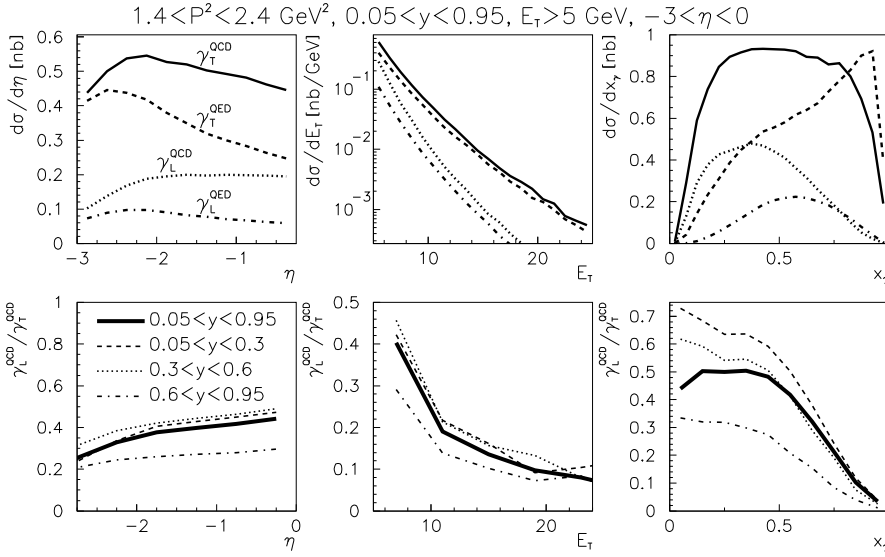


**Fig. 3.** The same as in Fig. 2, but for experimentally motivated restricted region  $-3 \leq \eta \leq 0$ .

we discard one common power of  $\alpha$  coming from the vertex where the virtual photon is emitted by the incoming electron. This vertex is also left out in diagrams of Fig. 6.

JETVIP contains full set of partonic cross sections for the direct photon contributions up the order  $\alpha\alpha_s^2$ . Examples of the corresponding diagrams are shown in Fig. 6a,b. To go one order of  $\alpha_s$  higher and perform complete calculation of the direct photon contributions up to order  $\alpha\alpha_s^3$  would require evaluating tree diagrams like that in Fig. 6e, as well as one-loop corrections to diagrams like in Fig. 6b and two-loop corrections to diagrams like in Fig. 6a. So far, such calculations are not available. In addition to complete  $\mathcal{O}(\alpha\alpha_s^2)$  direct photon contributions JETVIP includes also the resolved photon ones with partonic cross sections up to the order  $\alpha_s^3$ , exemplified by diagrams in Fig. 6c,d. The rationale for including in the resolved channel terms of the order  $\alpha_s^3$  is discussed in detail in [3]. Once

the concept of virtual photon structure is introduced, part of the direct photon contribution (which for the virtual photon is actually nonsingular) is subtracted and included in the definition of PDF of  $\gamma^*$ . To avoid misunderstanding we shall henceforth use the term “direct unsubtracted” (DIR<sub>uns</sub>) to denote NLO direct photon contributions *before* this subtraction, reserving the term “direct” (DIR) for the results *after* it. In this terminology the complete JETVIP calculations are given by the sum of direct and resolved parts and denoted DIR+RES. In JETVIP only the convolution of QED splitting term (plus some finite terms) corresponding to  $\gamma_T^*$

$$q_T^{\text{QED}}(x, P^2, M^2) = \frac{\alpha}{2\pi} 3e_q^2 (x^2 + (1-x)^2) \ln \frac{M^2}{xP^2}. \quad (5)$$

with  $\alpha_s^2$  partonic cross sections are subtracted from DIR<sub>uns</sub> calculations. We recall that in any NLO DIR<sub>uns</sub> calcula-

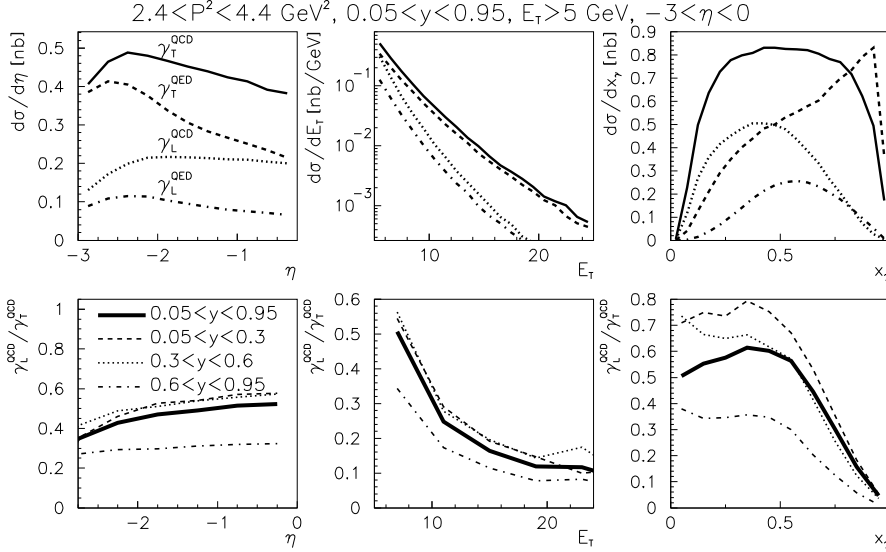


**Fig. 4.** The same as in Fig. 3 but for  $2.4 \leq P^2 \leq 4.4 \text{ GeV}^2$ .

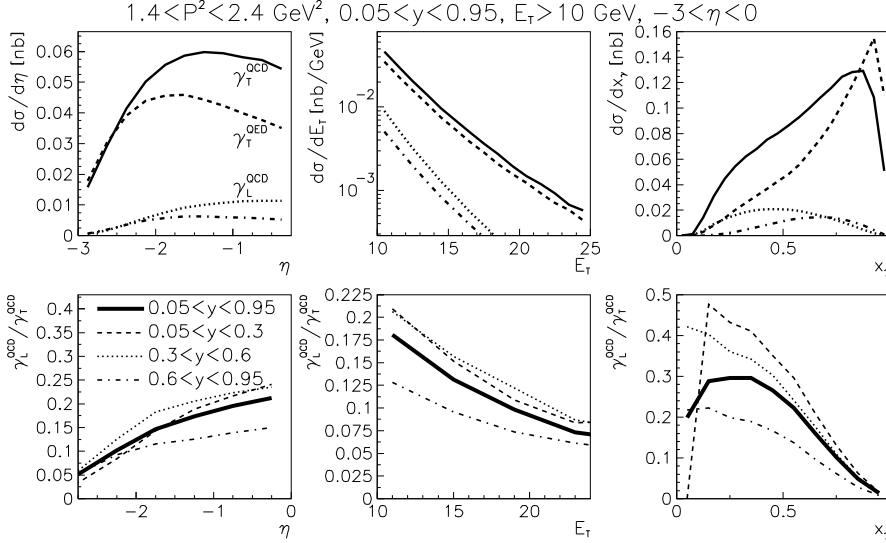


**Fig. 5.** The same as in Fig. 3 but for  $E_T = 10 \text{ GeV}$ .

tion both  $\gamma_T^*$  and  $\gamma_L^*$  are taken into account exactly up to the order  $\alpha_s^2$ . Introducing the concept of resolved  $\gamma_T^*$  and  $\gamma_L^*$  implies the replacement of the convolution (denoted  $\sigma(\text{PSP})$ ) of photon splitting terms ((5) for  $\gamma_T^*$  and (4) for  $\gamma_L^*$ ) and order  $\alpha_s^2$  partonic cross sections with the contribution (denoted  $\sigma_{T,L}(\text{RES})$ ) of the resolved  $\gamma_{T,L}^*$ . The net effect of this operation is thus the addition to  $\sigma(\text{DIR}_{\text{uns}})$  of the differences  $\Delta_{T,L} \equiv \sigma_{T,L}(\text{RES}) - \sigma_{T,L}(\text{PSP})$

$$\sigma(\text{DIR} + \text{RES}) = \sigma(\text{DIR}_{\text{uns}}) + \Delta_T + \Delta_L. \quad (6)$$

The appropriate measure of the relevance of resolved  $\gamma_L^*$  in NLO calculations is thus the ratio

$$r_{LT}^{\text{NLO}}(E_T, \eta) \equiv \frac{\Delta_L(E_T, \eta)}{\Delta_T(E_T, \eta)}. \quad (7)$$

Note that as for the LO QCD calculations the corresponding measure is the ratio  $\sigma_L(\text{RES})/\sigma_T(\text{RES})$ , the relevance

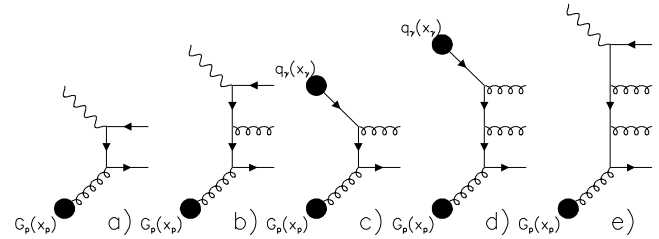


**Fig. 6.** Examples of diagrams contributing to dijet production in ep collisions at the orders  $\alpha_s$  (a),  $\alpha_s^2$  (b,c), and  $\alpha_s^3$  (d,e) taking into account that the upper blobs representing quark distribution functions of the photon are proportional to  $\alpha$ .

of  $\gamma_L^*$  in hard collisions is in general different at LO and NLO orders. For  $\gamma_L^*$  the cross section  $\sigma_L(\text{RES})$  is given by

the convolution of QCD improved PDF of  $\gamma_L^*$  with partonic cross sections up to the order  $\alpha_s^3$ .

To include the effects of resolved  $\gamma_L^*$ , we have modified JETVIP with the help from Björn Pötter in three places by adding:

- the flux (2) of  $\gamma_L^*$ ,
- the photon splitting term (4) corresponding to  $\gamma_L^*$ ,
- the call to PDF of  $\gamma_L^*$ .

We have checked our modifications against HERWIG as well as internally within JETVIP. In the first case we compared LO JETVIP results for  $\gamma_L^*$  with analogous results obtained with HERWIG 5.9 for the same QCD improved PDF of initial  $\gamma_L^*$ . Taking into account small differences between the way JETVIP and HERWIG

- set the scale of PDF and  $\alpha_s$ ,
- treat (light) quark mass effects,
- reconstructs kinematics from generated  $x_\gamma$ ,

we have found very satisfactory agreement in both shape and absolute normalization of resulting distributions in all three variables  $x_\gamma, \eta$  and  $E_T$ .

The modification of the photon splitting term (5) to the form appropriate for  $\gamma_L^*$  has been checked by comparing JETVIP results for  $\sigma_L(\text{PSP})$  with LO JETVIP results in the resolved channel obtained with purely QED expression (4) for light quark distribution functions. Apart from the opposite sign, the latter should be equal to the former as, indeed, it turned out to be the case to within a few %.

## 6.1 Hadronization corrections

Any meaningful comparison of JETVIP results with experimental data must involve estimates of the effects describing the conversion of partons to hadrons. These hadronization corrections are not simple to define, but adopting the definition used by experimentalists [14], we have found [11] that they depended sensitively and in correlated manner on the pseudorapidity and transverse energy of jets. For  $E_T^c = 5$  GeV, hadronization corrections become large and strongly model dependent for  $\eta \lesssim -2.5$ . We have therefore restricted our analysis to  $-2.5 \leq \eta \leq 0$ , where they are flat in  $\eta$  and do not exceed 10%.

## 6.2 Results

We have redone the calculation of [1] using QCD improved PDF of  $\gamma_L^*$ , but otherwise with the same assumptions concerning renormalization and factorization scales<sup>8</sup> and for identical kinematical region

$$-2.5 \leq \eta \leq 0, \quad E_T^{(1)} \geq 7, \quad E_T^{(2)} \geq 5 \text{ GeV}.$$

The resulting distributions  $d\sigma/d\eta$  and  $d\sigma/dE_T$  corresponding to the second window in  $P^2$  are shown in Fig. 7. We plot there separately all three contributions on the

<sup>8</sup> In PDF of  $\gamma_L^*$  we set  $A_{\text{QCD}}^2 = 0.1 \text{ GeV}^2$ .

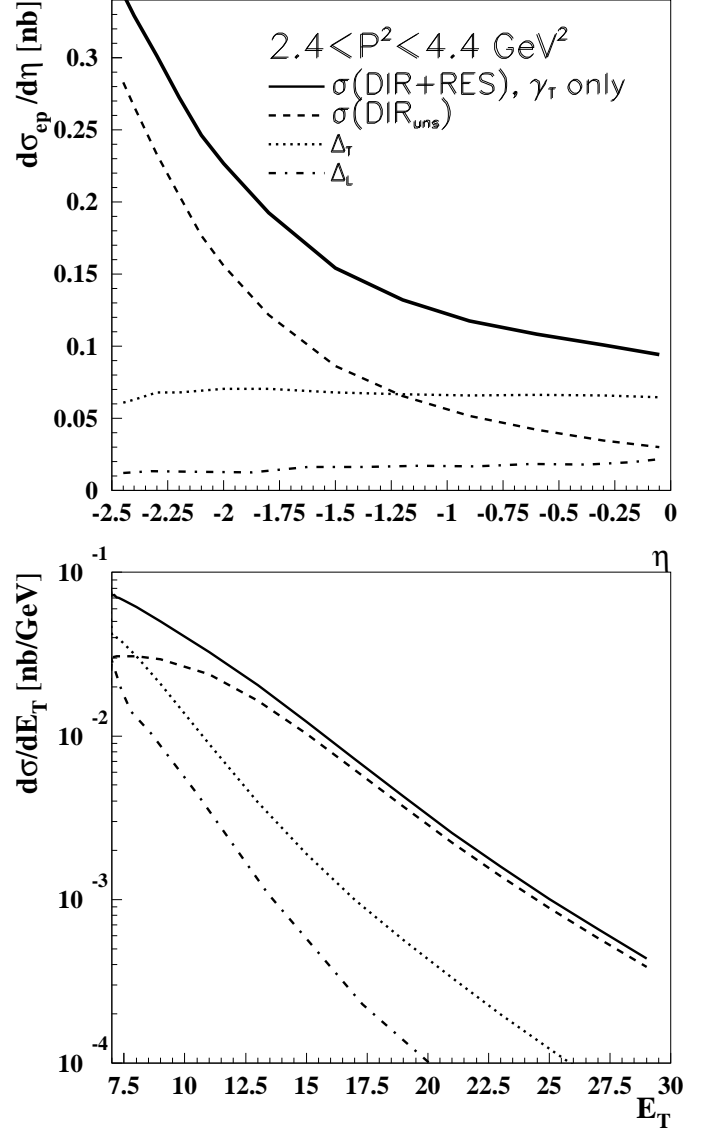


**Fig. 7.** Comparison of nontrivial parts  $\Delta_T$  and  $\Delta_L$  of the contributions of  $\gamma_T^*$  and  $\gamma_L^*$  to  $d\sigma/d\eta$  and  $d\sigma/dE_T$  distributions. The results of direct unsubtracted and full calculations using in the resolved channel  $\gamma_T^*$  only are shown as well.

r.h.s. of (6), as well as their sum defined in (6) but including the contributions of  $\gamma_T^*$  only. Note that both  $\Delta_T$  and  $\Delta_L$  are almost flat in  $\eta$  and rapidly falling in  $E_T$ , the latter fall-off being faster for  $\Delta_L$  as expected due to harder shape of PDF of  $\gamma_T^*$ . The resulting  $r_{LT}^{\text{NLO}}(E_T, \eta)$  rises slowly from about 0.2 at  $\eta = -2.5$  to 0.35 at  $\eta = 0$ , but decreases appreciably with  $E_T$ . Integrated over  $E_T$ , we find  $r_{LT}^{\text{NLO}}(\eta) \simeq 0.3$ , but for  $E_T$  close to the lower cut-off  $E_T^c = 7$  GeV, this ratio increases to about 0.5. Note also that for  $\eta$  close to  $\eta \simeq 0$ ,  $\Delta_L$  approaches the results of  $\text{DIR}_{\text{uns}}$  calculations.

Increasing the photon virtuality:

- reduces the relevance of resolved  $\gamma_T^*$  as measured by the ratio  $\Delta_T/\sigma(\text{DIR}_{\text{uns}})$ , but

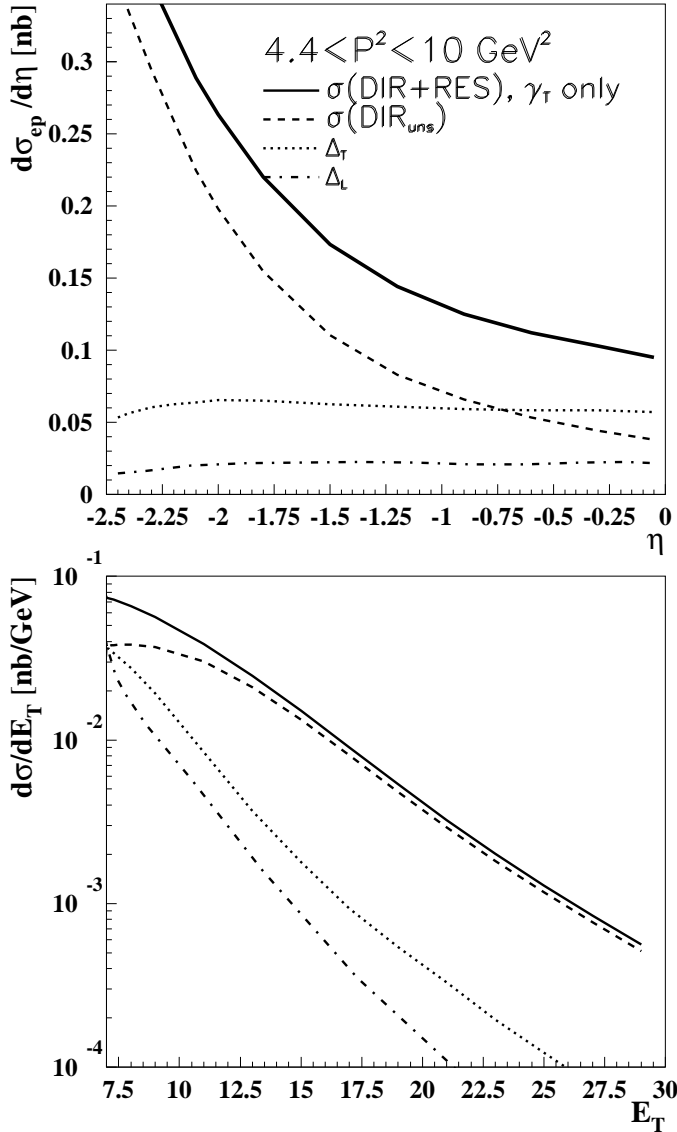


Fig. 8. The same as in Fig. 7 but for  $4.4 \leq P^2 \leq 10 \text{ GeV}^2$ .

– increases the relative importance of resolved  $\gamma_L^*$  with respect to resolved  $\gamma_T^*$  as measured by the ratio  $r_{LT}^{\text{NLO}}$ .

This is illustrated in Fig. 8, which shows the same plots as in Fig. 7 but for  $4.4 \leq P^2 \leq 10 \text{ GeV}^2$ . In this interval the mean value of  $r_{LT}^{\text{NLO}}$  is about 0.38, but for  $E_T$  close to  $E_T^c = 5 \text{ GeV}$  it approaches unity. Raising the cut-off  $E_T^c$  reduces the relevance of  $\gamma_L^*$  with respect to  $\gamma_T^*$ , for much the same reasons as in LO calculations.

In general, the relative importance of resolved  $\gamma_T^*$  and  $\gamma_L^*$  is determined by two circumstances: the presence of “large log”  $\ln(M^2/P^2)$  in PDF of  $\gamma_T^*$  and the difference in shapes of PDF of  $\gamma_T^*$  and  $\gamma_L^*$ . At very large value of the ratio  $M^2/P^2$  the first effect is clearly more important and leads to dominance of resolved  $\gamma_T^*$ . However, in presently accessible range at HERA this “large log” is fairly small number around 3 and thus the fact that PDF of  $\gamma_T^*$  are harder than those of  $\gamma_L^*$  plays equally important role.

Inclusion of the contributions of resolved  $\gamma_L^*$  in phenomenological analyses of HERA data on dijet production helps bring the theoretical predictions closer to the H1 data [11], but a thorough analysis of the evidence for resolved  $\gamma_L^*$  in current HERA data requires detailed discussion of a number of points, and is beyond the scope of this paper.

## 7 Summary and conclusions

We have analyzed the contributions of resolved  $\gamma_L^*$  to virtual photon structure function  $F_{\text{eff}}^\gamma$  and dijet cross sections measured at HERA, using the recently constructed parameterization of QCD improved PDF of  $\gamma_L^*$ . The contributions of resolved  $\gamma_L^*$  were shown to be nonnegligible with respect to those of  $\gamma_T^*$ , but their relevance depends on the order of QCD calculations employed and kinematical region considered. Within the LO QCD and in the kinematical regions accessible at LEP and HERA, they amount typically to 40 – 50% of those coming from resolved  $\gamma_T^*$ , but in parts of phase space (small  $y$  and  $x_\gamma$  or low  $E_T$ ) this number is even larger. Within the NLO calculations of virtual photon interactions the relative importance of  $\gamma_L^*$  with respect to  $\gamma_T^*$  is smaller, but still clearly of phenomenological relevance. In both cases the effects of QCD improved PDF of  $\gamma_L^*$  are clearly observable.

We are grateful to J. Cvach, C. Friberg and B. Pötter for interesting discussions concerning the structure and interactions of longitudinal virtual photons and to B. Pötter for help in modifying JETVIP. This work was supported in part by Grant Agency of the Academy of Sciences of the Czech Republic under the grants No. A1010821 and B1010005.

## References

1. J. Chýla, M. Taševský, Eur. Phys. J. **C16**, (2000) 471
2. J. Chýla, Phys. Lett. **B488**, (2000) 289
3. J. Chýla, M. Taševský, Phys. Rev. **D62**, (2000) in print, hep-ph/9912245
4. G. Schuler, T. Sjöstrand: Z. Phys. **C68**, (1995) 607  
G. Schuler, T. Sjöstrand: Phys. Lett. **B376**, (1996) 193
5. C. Friberg, T. Sjöstrand, Eur. Phys. J. **C13**, (2000) 151
6. C. Friberg, T. Sjöstrand, LU TP 00-31, hep-ph/0009003
7. J. Chýla, JHEP**04**, (2000) 007
8. M. Acciari et al. (L3 Collab.), Phys. Lett. **B483**, (2000) 373
9. G. Abbiendi et al. (OPAL Collab.), Eur. Phys. J. **C11**, (1999) 409
10. C. Adloff et al. (H1 Collab.), Eur. Phys. J. **C13**, (2000) 397
11. M. Taševský, PhD Thesis, Charles University, Prague, <http://www-h1.desy.de/psfiles/theses/h1th-181.ps>
12. B. V. Combridge, C. J. Maxwell, Nucl. Phys. **B239** (1084), 429
13. B. Pötter, Comp. Phys. Comm. **119**, (1999) 45
14. M. Wobisch, in *MC generators for HERA Physics*, Hamburg 1999, p. 239, hep-ph/9905444